Materials Science and Engineering C 59 (2016) 585–593

Contents lists available at ScienceDirect

Materials Science and Engineering C

journal homepage: www.elsevier.com/locate/msec

Mesoporous silica sub-micron spheres as drug dissolution enhancers: Influence of drug and matrix chemistry on functionality and stability

Laura Brigo [a,b], Elisa Scomparin [c], Marco Galuppo [c], Giovanni Capurso [e], Maria Grazia Ferlin [c], Valentina Bello [d], Nicola Realdon [c], Giovanna Brusatin [a], Margherita Morpurgo [c,*]

[a] Department of Industrial Engineering and INSTM Padova RU, University of Padova, via Marzolo 9, 35131 Padova, Italy
[b] Micro System Technology RU, Center for Materials and Microsystems, Bruno Kessler Foundation, via Sommarive 18, 38123 Trento, Italy
[c] Department of Pharmaceutical and Pharmacological Sciences, University of Padova, via Marzolo 5, 35131, Padova, Italy
[d] Department of Physics and Astronomy Galileo Galilei, University of Padova, via Marzolo 8, 35131 Padova, Italy
[e] Helmholtz-Zentrum Geesthacht, Institute of Materials Research - Dept. of Nanotechnology, Max-Planck-Strasse 1, D-21502 Geesthacht, Germany

ARTICLE INFO

Article history:
Received 16 July 2015
Received in revised form 30 September 2015
Accepted 12 October 2015
Available online 17 October 2015

Keywords:
Mesoporous materials
Nanoparticles
Microparticles
Drug dissolution enhancement
Anticancer oral therapy
Sol–gel process

ABSTRACT

Mesoporous silica particles prepared through a simplified Stöber method and low temperature solvent-promoted surfactant removal are evaluated as dissolution enhancers for poorly soluble compounds, using a powerful anticancer agent belonging to pyrroloquinolinones as a model for anticancer oral therapy, and anti-inflammatory ibuprofen as a reference compound. Mesoporous powders composed of either pure silica or silica modified with aminopropyl residues are produced. The influence of material composition and drug chemical properties on drug loading capability and dissolution enhancement are studied. The two types of particles display similar size, surface area, porosity, erodibility, drug loading capability and stability. An up to 50% w/w drug loading is reached, showing correlation between drug concentration in adsorption medium and content in the final powder. Upon immersion in simulating body fluids, immediate drug dissolution occurred, allowing acceptor solutions to reach concentrations equal to or greater than drug saturation limits. The matrix composition influenced drug solution maximal concentration, complementing the dissolution enhancement generated by a mesoporous structure. This effect was found to depend on both matrix and drug chemical properties allowing us to hypothesise general prediction behaviour rules.

1. Introduction

Scarce solubility of bioactive compounds is an important issue in pharmaceutical sciences since it has a negative impact on bioavailability and efficacy. Given that poor solubility is a common feature for many active molecules, several approaches have been suggested to improve their dissolution. Most of these rely on colloidal complex systems that act by enhancing the local solubility of the complexed drug — e. g. inclusion complexes, microemulsions, self-emulsifying drug delivery systems, solid solutions and dispersions, and salt formation [1–6]. More recently, an alternative/complementary strategy to implement drug availability has originated from the use of mesoporous silica-based materials. Such inorganic powder materials are characterized by a very large surface area, allowing for the adsorption of large amounts of drugs, which display enhanced dissolution thanks to the stabilization of their amorphous state and the large surface area available for the process [7,8]. These materials were originally developed as catalysts by Mobile (MCM41 = Mobile Composition of Matter 41) [9] but their use has expanded to several other areas, including the pharmaceutical industry [8]. Since the pioneering work of the group of Vallet-Regi in 2001, several papers have demonstrated the usefulness of diverse types of mesoporous silica, prepared through different routes, in improving drug dissolution [7–15]. Mesoporous silica is characterized by a stable and rigid framework, an ordered pore network, a large surface area and a pore volume which can change depending on the type of template used in the synthesis [8,16–18]. The pore network is generated by the polymerization of silica around cetyltrimethyl ammonium bromide (CTAB-MCM-41) [9] or PPO (SB-15) [19] micelles and by successive template removal, achieving pore diameters in the 2–6 nm range for MCM-41 and 4–13 nm range for SBA-15.

Classically, these materials are obtained through a high pressure condensation step, which is followed by calcination to remove the organic template. The resulting powders have a non-homogenous shape, while the calcination step does not permit inserting organic functional residues during the synthesis process. As a consequence, if organic functional residues need to be inserted onto the silica surface additional synthetic steps [20] are to be performed.

Here we investigated the potentials of a kind of mesoporous MCM41 sub-micron sized particles obtained through a low temperature Stöber-

* Corresponding author.
E-mail address: margherita.morpurgo@unipd.it (M. Morpurgo).

http://dx.doi.org/10.1016/j.msec.2015.10.039
0928-4931/

like synthetic process [21–23], in which template removal is achieved through a HCl/EtOH washing procedure, bypassing calcination [24]. This method, which was introduced by Etienne [24] in 2001, not only generates mesoporous materials directly in round-shaped particles, but also allows inserting organic moieties in the silica network directly along the one step synthetic process. So far, this kind of matrix has not been investigated as a pharmaceutical excipient. In this work, the potential of these MCM41 materials has been addressed through a series of experiments in which we evaluated a) if and how the spheres are capable of acting as dissolution enhancers for poorly soluble drugs; b) if and how the presence of an alkylamino function in the silica network and the drug chemical properties (namely the hydrophobic, and ionisable residues) affect the drug adsorption and dissolution enhancement properties; and c) if the material's properties are preserved along storage.

To this end, we selected two poorly soluble drugs as model compounds: the first one is a cytotoxic compound, 7-phenyl-3*H*-pyrrolo [3,2-*f*]quinolin-9(6*H*)-one (MG-2477), characterized by high potency [25,26] but very low solubility. It is a non-ionic molecule and – as the majority of anticancer compounds – it is characterized by extremely poor solubility in an aqueous environment. Indeed, despite the strong biological activity of this class of compounds, their hydrophobic nature generally leads to poor aqueous solubility and low bioavailability. For this reason they are normally administered through the slow infusion of large volumes of low concentrated solutions. Recently, the oral administration of anticancer agents (anticancer oral therapy — AOT) has also been investigated and, indeed, there has been an increase in the number of approved oral drugs for cancer therapy. AOT is in principle more convenient and allows better patient compliance. However, in order for it to be successful, immediate bioavailability of the active compound after oral administration is necessary, thus necessitating improving the slow dissolution profile. In particular, MG-2477 is a powerful chemotherapeutic molecule, acting mainly through the inhibition of tubulin polymerization, that displays strong cytotoxicity towards fast replicating cells, but low toxicity for resting ones [25,26]. Its antiproliferative properties make it a good candidate for use in anticancer oral therapy, therefore justifying the search for an oral formulation strategy capable of improving its bioavailability after administration.

The second drug is ibuprofen ((RS)-2-(4-(2-methylpropyl) phenyl)propanoic acid), an acidic (pKa = 4.49) poorly soluble compound that has often been used as a model in mesoporous silica gel investigations [10,11,14,27,28]. The two drugs display opposite pH dependence in their solubility behaviour, namely ibuprofen is more soluble in a neutral–basic environment, whereas MG-2477 is more soluble in an acidic solution (see Supplementary data). By using in parallel these two drugs with both pure mesoporous silica and amino-functionalized mesoporous silica particles, we investigated the effect of both the drug and the matrix chemical properties on the drug adsorption and dissolution behaviour. In addition, we performed a preliminary investigation on the effect of storage on the stability of the matrices, before and after drug adsorption, in view of a potential industrial application.

2. Materials and methods

2.1. Materials and instrumentations

Hexadecyl-trimethyl-ammonium bromide (CTAB) (99+%) and tetraethoxysilane (TEOS) were obtained from ACROS (Geel, Belgium). Ammonia solution (NH_4OH) (30 wt.%), 3-aminopropyltriethoxysilane (APTES), and all other chemicals were purchased from Sigma-Aldrich (St. Louis, MO). Double-distilled grade water was used in all experiments, except for matrix erosion assays, which were carried out in ultra-pure water obtained by inverse osmosis (milli-Q grade). FUI-grade ibuprofen was obtained from FRANCIS (Varese, IT). Ibuprofen concentration in aqueous buffers was determined by UV–vis analysis (264 nm) (Varian Cary 50) on the basis of calibration curves measured for each investigated buffer. The detection limit was about 100 μg/ml.

MG-2477 was synthesized at the Department of Pharmaceutical and Pharmacological Sciences (Dr. Ferlin lab) of the University of Padua. MG-2477 is a strongly fluorescent compound and its concentration in solution was assessed by means of fluorescence measurements (λ_{exc} = 272 nm, 5 nm bandwidth, λ_{em} = 495 nm, 10 nm bandwidth) (Jasco FP 6200) on the basis of calibration curves experimentally obtained. The detection limit was below 100 ng/ml.

2.1.1. XRD

X-ray diffraction patterns (XRD) were registered on a Bruker AXS D8 Advanced X-ray (Bruker, Germany) diffractometer, with a copper Kα radiation (0.15418 nm). Angular scans in the 1.5–9° range were collected with a step size of 0.02° using 100 mg samples of mesoporous powder.

Fourier Transform Infrared (FT-IR) absorption spectra of mesoporous powders dispersed in KBr were recorded in the 4000–400 cm^{-1} range by Fourier transform infrared spectroscopy (FT-IR) (Jasco FT/IR-620.) with an accuracy of 4 cm^{-1}.

Surface area and porosity properties were calculated starting from nitrogen adsorption-desorption isotherms obtained at 77 K, using a Quantachrome Autosorb iQ. Samples were degassed at 120 °C for at least 12 h under vacuum (before starting data acquisition, all samples displayed a pressure variation lower than 5 mTorr in a 15 min interval). For each sample three different batches of powder were measured, obtaining definitely compatible results within the experimental error. Nitrogen absorption isotherm data were analysed by the BET (Brunauer–Emmett–Teller) method to retrieve the specific surface area [29], and the plots of the corresponding pore size distribution were obtained from the desorption branches of the isotherms by using BJH (Barrett–Joyner–Halenda) model [30] and from a NLDFT (non-linear density functional theory) model applied to the adsorption branches [31,32].

TEM analysis has been performed with a Jeol 3010, operating at 300 kV equipped with a Gatan slow-scan CCD camera (Mod. 794), in order to investigate the film structure. S-TEM analysis has been performed at CNR-IMM Institute (Bologna, Italy) with a field-emission gun (FEG) scanning microscope (FEI Tecnai F20 Super Twin) operating at 200 kV with an electron beam size of about 1 nm FWHM and equipped with an high-angle annular dark field (HAADF) detector.

2.2. Synthesis of mesoporous silica

Mesoporous silica particles were obtained at room temperature through the ammonia-catalysed hydrolysis of alkoxysilanes in the presence of CTAB as the template. A typical synthesis involved the dissolution of CTAB in a round bottom flask in a water:ethanol:30% ammonia (100:100:25 volume ratio) mixture, to a final concentration of 21 mg/ml (5.8 mM), followed by the addition of the alkoxysilane precursor(s). After 2 h stirring at room temperature, the resulting solution was centrifuged for solid precipitation. Powders were washed with water, then with absolute ethanol, dried under vacuum, and finally heated at 70 °C for 3 h. Template removal was performed suspending powders in a 1 M solution of HCl in ethanol (1 g/100 ml) and stirring for 24 h at room temperature. Such mixtures were centrifuged, the solvent removed, the powders dried under vacuum and analysed by FT-IR spectroscopy. This procedure was repeated until the characteristic CTAB IR absorption bands in the spectral range of 2900–2800 cm^{-1} progressively disappeared.

Two different types of powders were obtained: 1) a silica-based system, in which only TEOS was used as an alkoxysilane precursor ("T" formulation), and 2) an amino-functionalised silica-based matrix ("TA" formulation), in which TEOS and APTES were used as precursors in 90:10 M ratio. For the TA formulation, the two synthesis precursors were mixed together in a separate vessel prior to addition to the CTAB

solution. In all syntheses, 0.142 mmol of alkoxysilane were added to each ml of CTAB solution. The amounts of reagents used for the preparation of 1 g of final powder are summarized in Table 1. The final formulations were also tested via the ninhydrin test. The positive blue colouration was observed on the surface of TA powders only, thus confirming the incorporation of primary amines in this formulation [33].

2.3. Matrix erosion

MCM-41 matrix erosion was investigated by immersing the powders (5 mg) into 10 mM tris hydroxymethylaminomethane, 150 mM NaCl, pH 7.4 (TRIS) buffer at 37 °C, in a shaking water bath. The ratio between matrix and buffer was 1 mg/8 ml, and was selected to avoid reaching silicic acid saturation in the medium (2 mM) [34,35]. At scheduled times, small fractions of the solution (800 μl) were removed for silicic acid quantification and replaced by fresh buffer. Silicic acid concentration was quantified using the molybdenum-blue colourimetric test [36]. Erosion data were mathematically elaborated and were plotted as (Mt/Mtot)% vs time, where Mt is the amount of silica released at time t, and Mtot is the total silica contained in the sample. Tests were performed the day after gel preparation and thirty days later, to verify the stability of the formulations upon storage (in closed vials and at room temperature).

2.4. Matrix loading with MG-2477 and ibuprofen

Drugs were adsorbed using the "immersion method" [16]. Several organic solutions with different concentrations of ibuprofen in dry ethanol and MG-2477 in dry dimethylsulfoxide (DMSO) were generated (Supplementary data, Table S-2). The mesoporous powders were immersed at room temperature in such solutions under gentle mixing. The ratio between the powder and the organic solution was kept constant at 40 mg/ml in all experiments. After overnight incubation, mixtures were centrifuged (16,600 *g*, 10 min, room temperature) and the supernatant removed. In order to remove non-physisorbed molecules (and in the case of MG2477 samples, DMSO residuals) powders were quickly treated with ethanol/methanol (vortexing 50 mg of powder/ml of solvent for 10 s), which was removed after centrifugation (16,000 *g*, 1 min, room temperature). Due to the risk of removing also physisorbed drug molecules with the washing step, the conditions of this procedure (volume ratios, timings and temperatures) were strictly controlled and kept constant for all samples. Powders were finally dried under vacuum. Several loading experiments were carried out using varying the drug concentration in solution in the 4–400 mg/ml range (Supplementary data, Tables S-2 and S-3).

Drug load was assessed by immersing small aliquots of the adsorbed samples (in the 5–120 mg range, depending on the drug and its load — Tables S-2 and S-3 in the Supplementary data) in organic solvent (0.2–1 ml) (ethanol for ibuprofen and methanol for MG-2477). After overnight incubation, the organic solution was removed by centrifugation and analysed for drug content. The same procedure was repeated until total powder exhaustion.

Table 1
Amounts of reagents used in the preparation of T and TA powders.

	T	TA
CTAB solution (ml)	113	113
TEOS (ml)	3.47	3.11
APTES (ml)		0.38
Final solution (ml)	116.47	116.49
TEOS:APTES:H_2O:CTAB	1:0:178.6:0.42	0.9:0.1:179.6:0.43

2.5. Drug dissolution

Drug dissolution was followed at 37 °C using a shaking water bath. The drug loaded powders (17.7% w/w in ibuprofen and 13.3% in MG2247) were added to the buffer solution (30 mL) and at scheduled times, 1 ml of the medium was removed for drug quantification and replaced with fresh buffer. In order to minimize material losses, the aliquots were centrifuged (16,600 *g*, 1 min, 37 °C) prior to analysis and the residue at the bottom of the microtube was re-suspended into the replacing fresh buffer aliquot. Dissolution experiments were carried out in 0.1 M HCl (the medium indicated by the pharmacopoeia to simulate the acidic gastric environment) or the physiological 10 mM phosphate, 150 mM NaCl, pH 7.4 (PBS) for ibuprofen or MG-2247, respectively, namely the pH conditions in which each drug displays lower solubility (see Supplementary data). We carried out different assays varying the ratio between drug loaded powder and dissolution medium, in order to reach a maximal drug concentration in the case of total dissolution equal to 2 or 4-fold its saturation (see Supplementary data). Dissolution data were mathematically elaborated and were plotted as either (C/Cs) or (Mt/Mtot)% vs time, where C is concentration measured at each time point and Cs is the saturation concentration, and Mt and Mtot are the amounts of drug dissolved at time t and the total available in the dissolution process.

Drug concentration in the release medium was determined by UV spectrophotometry at 272 nm (ibuprofen) or by fluorescence spectrometry (MG2477, $\lambda_{exc} = 274$ or 245 nm; $\lambda_{em} = 495$ nm) according to calibration curves obtained in parallel.

3. Results

3.1. TEM analysis

Fig. 1 shows the TEM images of the two formulations. The average particle size is 1.0 ± 0.3 μm for the T formulation, and 0.7 ± 0.2 μm for TA. A mesoporous structure is evident in both powders with a mean pore size of about 3–4 nm. XRD measurements (Fig. 1C) show the presence of a sharp peak at 2.4° and of weaker peaks at 4.1° and 4.8°, more pronounced in the T powder and barely visible in the TA one, which suggest that the mesopores are organized in ordered domains with hexagonal lattice (a structure similar to that reported in [23,24]). In order to better analyse the mesostructure of powders we have used high-angle annular dark field scanning TEM (HAADF-STEM) that has demonstrated to be a powerful technique for characterizing mesopores, as the contrast of the image is strongly correlated with local atomic number and therefore with the local atomic density [37]. The presence of radially-aligned pore channels and of small craters on the surface is visualized in T amorphous spheres (Fig. 1D). Fast Fourier transform (FFT) analysis of the STEM images revealed the presence of an ordered pore structure in the T powders with a periodicity of 3.5 ± 0.5 nm (inset of Fig. 1D). TA amorphous spheres show a more regular surface with respect to T spheres: no surface craters and no pore channels are observed in STEM images (Fig. 1E).

3.2. BET

Nitrogen (N_2) adsorption/desorption isotherms are shown in Fig. 2. Both samples display the shape of a Type IV isotherm, typical of a mesoporous silica as MCM-41 [5,6]. The T sample demonstrated an hysteresis loop in the adsorption/desorption cycle, that became much wider in the case of TA samples, for which an H2-type loop can be identified according to the IUPAC classification [38]. BET surface areas were determined from nitrogen isotherms at 77 K in a range of relative pressures (p/p_0) prior to the occurrence of pore condensation for each sample (T: 0.12–0.27; TA: 0.1–0.22) by assuming a cross-sectional area of 0.162 nm^2 for N_2. The BET surface values are reported in Table 2.

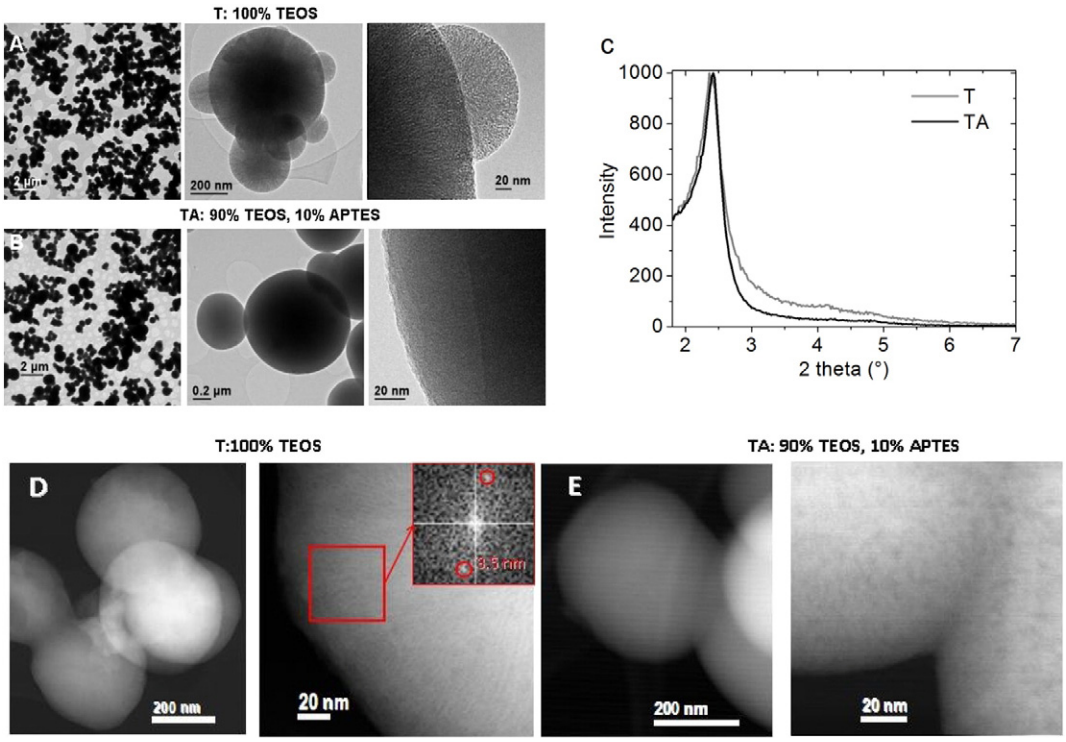

Fig. 1. TEM images of (A) T and (B) TA powders. (C) X-ray diffraction pattern of the T (grey line) and TA (black line) formulations. The presence of a sharp peak at 2.4° suggests a long range hexagonal order for the mesopores. HAADF-STEM images of (D) T and (E) TA powders. In the red square FFT analysis of the indicated area is reported: the symmetric spots correspond to an ordered pore structure with a periodicity of 3.5 nm. The figure shows representative images from one batch; analogue results were obtained from the other two batches.

In order to determine the pore size distribution (PSD), two different approaches were followed: a thermodynamic approach based on the Kelvin equation (BJH model) and a NLDFT method. Two different analyses were necessary because, for TA samples, the desorption branch closed the hysteresis loop showing a possible cavitation effect, which is known to create an artefact in the BJH estimates of PSD [39]. Such an effect is clearly visible in the inset of Fig. 2B, where data from the BJH model returns a second fictitious peak, corresponding to pores of larger diameter.

The NLDFT distribution displays only one peak for both samples, in the early mesopores range: the difference in pore diameter obtained with the two different approaches is widely discussed in literature [39,40].

Using data from BET and BJH analyses in Table 2, and NLDFT results only as a confirmation of the unique presence of mesopores with a size close to 2 nm, the two samples appear very similar in terms of surface and pore quantitative properties. The main difference between the two types of produced powders can be found in the different size of the hysteresis, indicating a more interconnected pore network for TA powders. The size of the pores is enough to create bottlenecks in the material network, which can also determine to the mentioned cavitation effect.

3.3. FT-IR analysis

FT-IR spectra of the T and TA powders were registered the day after synthesis and after 30 days of storage at room temperature in closed vials. The spectra of Fig. 3 reveal a complete removal of the surfactant (CTAB) for the absence of characteristic C–H stretching peaks in the 3000–2700 cm^{-1} region. In TA samples, N–H bending vibrations and N–H wagging weak peaks are present at 1517 cm^{-1} and at 700 cm^{-1}, respectively. The main difference between T and TA spectra is the position of Si–O–Si stretching at 1095 and 1080 cm^{-1} for T and TA

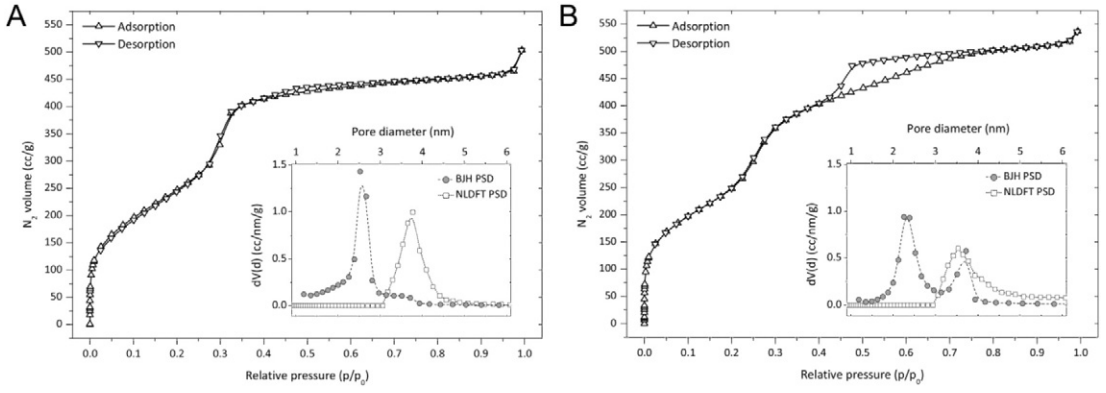

Fig. 2. N_2 isotherms for T particles (A) and TA particles (B) and, in the insets, their pore size distributions. The plots show data from one batch but analogue results were obtained from the other two batches.

Table 2
Surface and pore analysis results.

	S from BET (m^2/g)	Pore V from BJH (cm^3/g)	Pore Ø from BJH (nm)	Pore Ø from NLDFT (nm)
T	1011	0.917	2.526	3.775
TA	1013	0.945	2.257	3.537

respectively. The difference indicates that a more condensed silica network is present in the former (Fig. 3A'). Moreover, the spectra measured after 30 days (Fig. 3B and B') indicate a water up-take particularly evident for TA and negligible in the case of T powders, as revealed by the increased –OH absorption band at 3600–3200 cm^{-1} and the H_2O peak at 1650 cm^{-1}.

3.4. Matrix erosion

The erosion profiles of the two formulations when immersed in physiological buffer at 37 °C are shown in Fig. 4. Erosion was tested the day after powder synthesis and after 30 days of storage.

Silica in aqueous solution dissolves into silicic acid. This compound has limited solubility and its saturation in water or aqueous buffers is about 2 mM [34,35]. In order to avoid any bias in the dissolution experiment due to the risk of reaching saturation of silicic acid, the volume of the acceptor solution was selected in order to allow full dissolution of the silica contained in the sample (*sink* conditions for silicic acid). The results show that both samples dissolve very rapidly and 100% dissolution occurs within the first 5 h. No apparent difference was observed between the two preparations when analysed the day after preparation, indicating that the presence of 10% aminopropyl modified silicon centres does not influence the dissolution. However, only the T formulation maintained the same dissolution profile after 30 days of storage. On the contrary, the dissolution profile of TA was about 10% slower after the storage, suggesting some instability in this matrix structure.

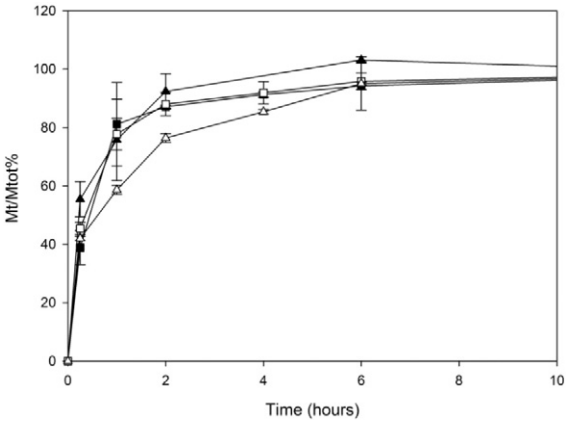

Fig. 4. Erosion profiles of T (□) and TA (Δ) matrices as measured the day after preparation (full symbols) and after 30 days of storage at room temperature in a closed vial (empty symbols).

3.5. Drug loading and dissolution

Fig. 5 displays the relation between both ibuprofen and MG-2477 concentration in the adsorption solution and their content in the final formulation (see also Table S-2 in Supplementary data). A similar trend in drug load vs adsorption solution concentration can be observed, independently of the drug and the matrix composition. The maximal drug content achieved on both T and TA was >50% w/w for ibuproben adsorbed from a 400 mg/ml solution and about 2.5% w/w for MG-2477 adsorbed from a 40 mg/ml solution. In this case, adsorption experiments from higher concentrated solutions could not be carried out due to drug availability limits.

The adsorption properties for ibuprofen are in line with those described in the literature for MCM41 mesoporous materials obtained through alternative routes [35,41], also considering the

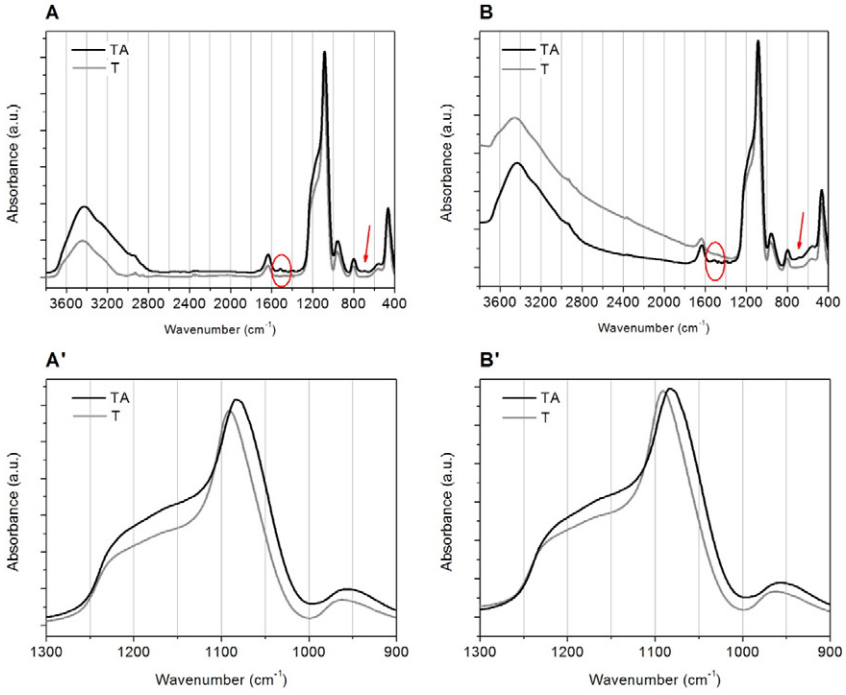

Fig. 3. FT-IR spectra of T and TA powders immediately after CTAB removal (A) and after 30 days of storage at room temperature (B). The circles and arrows indicate the N–H stretching and wagging, respectively. Respective zoomed spectra of the silica peaks (A', B').

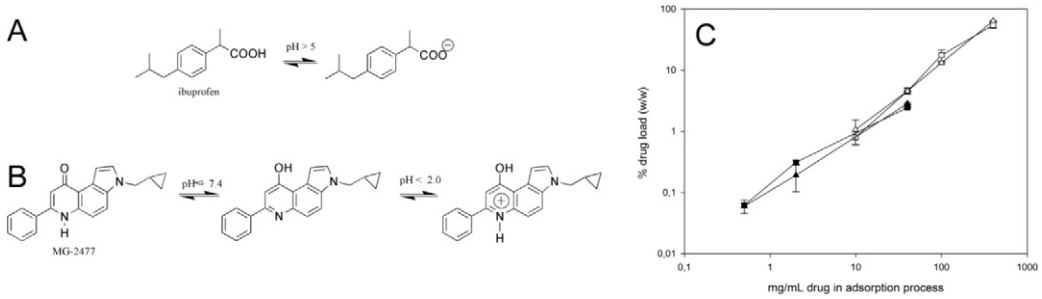

Fig. 5. Chemical structures at different pH values of A) ibuprofen and B) MG-2477 and C) correlation between their concentration in the adsorption solution and final matrix loading. (■,□) Formulation T and (▲, Δ) formulation TA. Open symbols: ibuprofen, full symbols: MG-2477.

high dependence of this parameter on the loading procedure and conditions adopted [17].

Data of Fig. 5 were obtained by carrying out the adsorption process using freshly prepared mesoporous powders. In addition, ibuprofen adsorption at 100 mg/ml was repeated on matrices stored in closed vials for 30 days at room temperature in order to evaluate the effect of matrix storage upon this parameter. The results are shown in Table 3. The loading capability of both mesoporous formulations decreases upon storage, and this loss is more pronounced for TA (57%) than T (48%).

XRD measurements on final ibuprofen-loaded formulations (Fig. 6) demonstrate that matrix structure and pore arrangement were preserved after the loading process: the peak at 2.4 was still present, even if slightly shifted to higher angles for T particles. The absence of ibuprofen diffraction peaks in the spectra show that the mesopores entrap the drug in its amorphous form.

The results of the drug dissolution experiments are depicted in Fig. 7. The release data are expressed both as Mt/Mtot% vs time and as C/Cs vs time. The latter plot provides additional information to the more classic Mt/Mtot% one. In fact, the % of drug dissolution can be affected by the acceptor solution volume, in particular when the experiments (as here) are carried out in nonsink conditions for the drug, so that 100% dissolution cannot be reached due to physical limits. In this case, expressing the release profile through the ratio between the actual drug concentration and its saturation concentration better highlights the solubility enhancement promoted by the mesoporous system.

All formulations were capable of delivering the drug in the dissolution medium much faster than when the drugs were tested as such. In all formulations the maximal drug concentration was reached within 5 min, as opposed to when testing the pure drugs, which required more than 90 min to reach saturation concentrations. Dissolution enhancement occurred independently of the drug or matrix chemical properties. However, significant differences were registered in the maximal solution drug concentration reached by the different formulations. In the case of ibuprofen, when the drug was adsorbed on the T pure silica matrix, its concentration in the dissolution medium never exceeded the saturation level (C/Cs = 1). On the contrary, when adsorbed onto the amino modified matrix, the drug concentration in the early phase of the dissolution reached well above saturation (up to 2.5 fold) levels. However, after the initial burst, drug concentration slowly went down secondary to precipitation. A similar phenomenon with an opposite trend was observed with MG-2477, for which the highest solution concentration was reached when the drug was adsorbed onto the pure silica T formulation.

Table 3
Matrix loading capability for ibuprofen from 100 mg/ml ethanol solutions as a function time of storage at room temperature. Loading experiments was carried using the powders as such (*) or after overnight treatment at 80 °C (**).

Ageing	T	TA
	Ibuprofen/SiO_2% w/w	
Freshly prepared	19.91 ± 2.85	13.46 ± 1.45
30 days	(*) 10.37 ± 1.08	(*) 5.82 ± 0.08
	(**) 12.20 ± 0.56	(**) 8.43 ± 1.29

3.6. Stability of drug-loaded formulations

Preliminary investigation on formulation stability was carried out. Dissolution from the same ibuprofen loaded formulation was tested the day after preparation and 40 days later, upon storage in a closed vial at room temperature. As shown in Fig. 8, the enhanced dissolution profile was preserved by both T and TA matrices, indicating that both final formulations are indeed stable.

4. Discussion

4.1. Selection of the silica mesoporous formulations

The usefulness of mesoporous silica powders as solubility enhancers for poorly soluble drugs has already been demonstrated in several contexts [7,8]. The aim of this work was to contribute to this field of investigation by studying the potentials of mesoporous particles obtained through a low temperature 'simplified' Stöber method. As demonstrated by TEM and BET (Figs. 1 and 2), the synthesis yields round-shaped sub-micron particles which are rather homogeneous in size, possess an ordered mesoporous structure and have a very large surface area. Thanks to the possibility of bypassing calcination, we could generate directly using one-step synthesis processes, mesoporous materials differing because of the presence or absence of organic (aminopropyl) moiety residues. In this way the influence of the matrix composition on functional properties could be investigated.

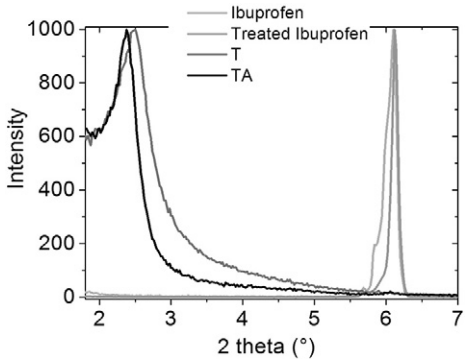

Fig. 6. X-ray diffraction spectra of the T (dark grey line) and TA (black line) formulations after loading with ibuprofen. Drug spectra as purchased, or after immersion in ethanol solution and drying, are reported for comparison (light grey lines).

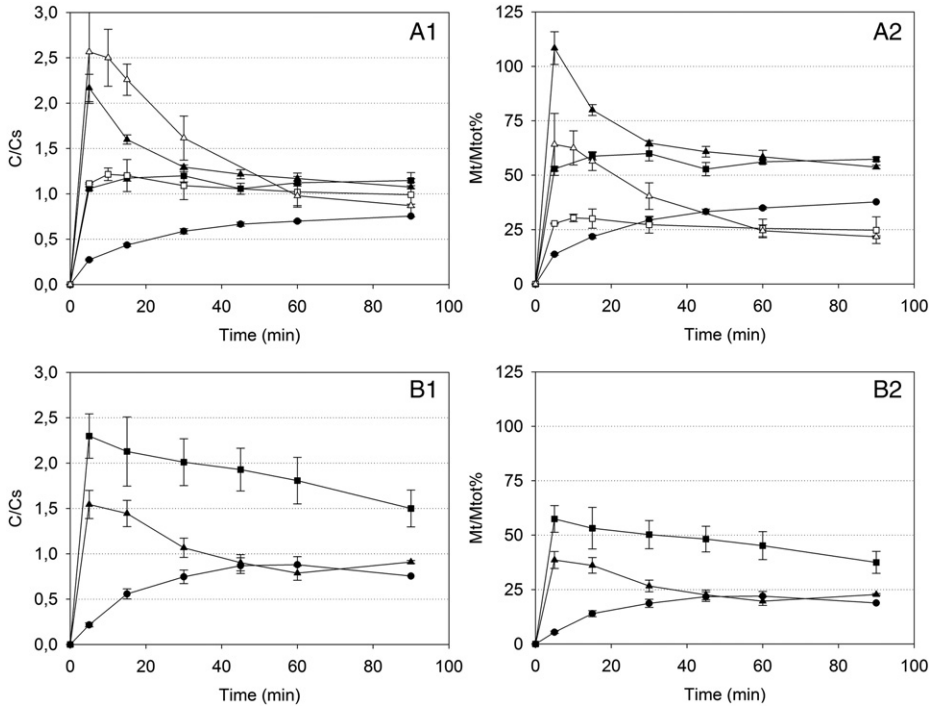

Fig. 7. Dissolution profiles of (A) ibuprofen in 0.1 M HCl and (B) MG-2477 in PBS buffer. Dissolution was carried out using drugs in their original powder (●) or adsorbed onto T (□, ■, square) or TA (▲, Δ, triangles) mesoporous silica. In the case of ibuprofen, dissolution assays were carried out using 0.2 mg (full symbols) or 0.4 mg (empty symbols) of drug/ml of acceptor solution (2× or 4× with respect to drug saturation concentration, respectively). In the case of MG-2477, assays were carried out using 1600 ng of MG-2477/ml of acceptor solution (4× saturation concentration). Dissolution data are plotted as (A1 and B1) drug concentration (C) divided by the drug saturation concentration (Cs) or (A2 and B2) as Mt/Mtot% vs dissolution time.

4.2. Adsorption and dissolution enhancement

Different methods can be used to load drugs onto mesoporous materials, including the use of filtration, slow evaporation, melting, spray-drying, or rotary evaporation [17]. Here, drug loading was achieved using the simple "immersion method", in which adsorption occurs upon overnight contact of the matrices with drug solutions, using organic solvents in which the compounds display high solubility. By performing the adsorption process at different solution concentrations, a relationship between solution concentration and drug load is obtained, whose trend provides an indication of the adsorption efficacy. Fig. 5B shows that a similar adsorption trend is obtained independently of the drug and matrix type, indicating that neither the drug chemical properties nor the presence of the 10% moles of aminopropyl residues in the silica network affect the material's high adsorption properties. These results are not obvious and differ from previous results obtained with similar formulations in which the aminopropyl function was introduced after the pore formation [20]. Indeed, aminopropyl residues were expected to bring steric hindrance and reduce the total surface area, or affect the pore structure and the drug adsorption features. In addition, their ionic property could influence drug adsorption through ionic effects. However, the combination of these data with the BET analysis indicates that it is the surface area available for the process that determines matrix adsorption potential, while the introduction of the aminopropyl function directly during matrix preparation, as in the here-adopted process, did not affect this parameter.

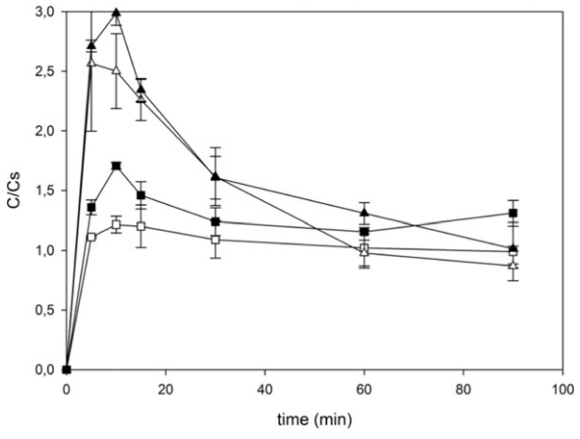

Fig. 8. Ibuprofen dissolution from T (■, □) and TA (▲, Δ) loaded matrices, tested the day after matrix loading (empty symbols) and upon 40 days of storage in closed vials at room temperature (full symbols). Dissolution tests were carried out in 0.1 M HCl using 0.4 mg of drug/ml of acceptor solution (4× with respect to drug saturation concentration).

All drug loaded formulations were capable of delivering the drug in the dissolution medium much faster than when the drug was tested alone, and maximal drug concentration (equal or above saturation levels) was always reached within 5 min of the dissolution test. As opposed, in the same conditions, the pure drugs required more than 90 min to reach similar saturation concentrations. The fact that the above saturation levels can be reached within a very short time is extremely relevant for bioavailability, as a higher concentration in the burst phase might likely translate into faster onsets of action.

Noteworthy, the dissolution kinetics observed appear to be faster than those described in the literature with MCM41 materials loaded with ibuprofen [42,35,43,20]. For example, round shaped particles prepared by Manzano et al. [20] using a similar procedure to the one here described but followed by calcination and loaded at about 25%–36% w/w with ibuprofen, showed a slower (equilibrium after 48–150 h) and incomplete ibuprofen release in simulating body fluid (SBF [44]), which was also affected by the presence of amino residues on the surface of the particles. Similarly, MCM41 spheres prepared by Onida et al. carrying 37% w/w ibuprofen [35], necessitated 2 to 10 h to reach

full drug dissolution in SBF, a time during which pore occlusion was also observed. However, it has to be noted that comparison with literature data is not always straightforward, either because the dissolution test conditions (e.g. ratio between drug and volume, which is – according to the Noyes–Whitney equation [45] – a fundamental parameter in determining a drug dissolution rate) are different or are not fully described [41,42], or because of differences in the drug loading and rinsing procedures before drying, or differences in the acceptor solution composition [35]. Another possible reason for the differences observed may be due to different observation timeframes: we concentrated our attention mostly on the early phase of the dissolution whereas other works, focusing also on later phases, did not report what was happening at the onset of the phenomenon. In any case, the materials described in this work appear to have more similar characteristics to those of irregularly shaped mesoporous MCM41 powders obtained through more classic procedures [20,9].

Even if dissolution enhancement was exhibited by all formulations and independently of the drug or matrix chemical properties, significant differences were observed in the maximal drug concentration reached in the dissolution medium (Fig. 7). This result can be explained considering that, depending on the matrix composition, the adsorbed drugs interact with it by their ionized form. The adsorbed form is the one that has the first contact with the dissolution medium and is readily extracted by it. Since drug desorption from the mesoporous surface is instantaneous, it is the solubility feature of the adsorbed form that dictates the solution concentration at the onset of the process. Consequently, if the adsorbed form is more soluble than the one that the compound acquires in the dissolution medium, solution concentrations higher than saturation can be reached. However, since drug solubility limits cannot be overcome for long, drug precipitation occurs with time until true saturation levels are reached. This explains the opposite effect exerted by the TA and T matrices – the first with basic features and the second slightly acidic – on the two drugs with different chemical properties. In the case of ibuprofen, the amino carrying matrix may adsorb the drug in the more water soluble carboxylate form. In the case of MG-2477, at high pH the molecule adopts two tautomeric forms, according to a keto-enol equilibrium (Fig. 5A). In particular, the enol form, which is protonable at low pH (data not shown), is more water soluble than the keto one. Therefore, the drug solution concentration reached upon T adsorption is higher than that reached upon adsorption on the amine carrying TA, in which the keto form is favoured.

From a practical point of view, we may expect this phenomenon to be of general value. This means that, in order to reach higher drug concentrations at the onset of the dissolution process, one should select the matrix that favours adsorption of the drug in its more soluble conformation. Therefore, for acidic ionisable compounds, such as ibuprofen, the ideal matrix will carry basic organic functions (e.g. amines as in TA), whereas for basic ionisable compounds, as MG-2477, the matrix should contain acidic organic functions (e.g. carboxyl, sulphates, etc.)

4.3. Stability upon storage

The stability of a drug formulation is fundamental for practical purposes. Investigation on stability is also important when developing novel excipients, as in this case. The experiments described here were aimed at evaluating, in a preliminary way, the stability parameter on both the matrices as such and on the final drug loaded mixtures.

The results on matrix dissolution (Fig. 4) and drug loading capability upon storage (Table 3) show that the pure matrices' properties change with time. However, the decrease in loading capability is likely due – or at least in part – to the adsorption of water, as demonstrated by the fact that this parameter is partially recovered upon overnight treatment at 80 °C. This is in line with the FT-IR data (Fig. 3) that reveal a higher tendency of the TA matrix to take up water. This instability can be controlled by improving the storage conditions, namely by using sealed containers. On the other hand, the change observed in the erodibility of the TA matrix also indicates, at least for this formulation, the occurrence of some silica network rearrangement, which may have concurred with the water uptake in reducing the loading potential. This phenomenon is often observed with nonthermally cured organically functionalised silica [46]. In this respect, further investigation should be carried out to rule out the risk of a matrix network instability before drug loading, and or to establish if and how the matrix can be stabilized, for example through a temperature induced curing step or by simply improving the storing conditions.

In any case, from a practical point of view, it is more important to evaluate if the final drug-loaded formulation is stable in time. Indeed, it appears that the instability observed before drug loading does not influence the dissolution enhancement property, since (Fig. 8) the final drug loaded formulations were stable upon storage. This result is of importance as it confirms that mesopore entrapment stabilizes the amorphous (and faster dissolving) form of the drug, as also shown by XRD data.

5. Conclusions

The data converge in indicating that the silica particles here investigated are promising excipients for formulating poorly soluble drugs, with properties that are compatible with their application as enhancers in anticancer oral therapy. Both mesoporous powders displayed very high loading capability and powerful dissolution enhancement properties. The synthetic method here adopted, which allows introducing organic moieties in the mesoporous silica network, was found to be useful. In fact, while the presence of organic functions does not alter the drug loading efficiency or the matrix solubility enhancement properties, the insertion of suitable organic residues is not inconsequential, as it affects the maximal drug concentration at the onset burst of dissolution. This effect complements the general dissolution enhancement property of mesoporous silica powders and may have important consequences on the final drug bioavailability. In addition, the possibility of inserting selected functional residues may also be used to convey additional properties to the material, for example to favour bioadhesion. An optimization of the synthetic method aiming to an improvement of particle homogeneity is required in the perspective of optimizing the preparation for industrial development. Despite that some matrix instability was observed in the case of the drug-free aminopropyl carrying powder, all drug-loaded formulations appear to be 'functionally' stable, that is they maintained their strong solubility promoting feature also upon storage. This is encouraging for future applications. As for the matrix loss in drug loading capability upon storage, a more detailed investigation is still needed to rule out the risk of irreversible network changes that, if not prevented, could impair industrial development.

Acknowledgements

The authors are grateful to Prof. G. Mattei and Prof. S. Polizzi for assistance in TEM and STEM analyses. The University of Padova is acknowledged for funding through Ex 60%. The CARITRO Foundation is acknowledged for funding through 2014 Scientific Research Projects for Young Researchers "Detection of residual antibiotics in milk based on plasmonic sensors integrated with microfluidic platforms".

Appendix A. Supplementary data

Supplementary data to this article can be found online at http://dx.doi.org/10.1016/j.msec.2015.10.039.

References

[1] M.E. Brewster, T. Loftsson, Cyclodextrins as pharmaceutical solubilizers, Adv. Drug Deliv. Rev. 59 (2007) 645–666.
[2] R.L. Carrier, L.A. Miller, I. Ahmed, The utility of cyclodextrins for enhancing oral bioavailability, J. Control. Release 123 (2007) 78–99.

[3] R.H. Muller, C. Jacobs, O. Kayser, Nanosuspensions as particulate drug formulations in therapy. Rationale for development and what we can expect for the future, Adv. Drug Deliv. Rev. 47 (2001) 3–19.
[4] M. Perrut, J. Jung, F. Leboeuf, Enhancement of dissolution rate of poorly soluble active ingredients by supercritical fluid processes. Part II: preparation of composite particles, Int. J. Pharm. 288 (2005) 11–16.
[5] S. Talegaonkar, A. Azeem, F.J. Ahmad, R.K. Khar, S.A. Pathan, Z.I. Khan, Microemulsions: a novel approach to enhanced drug delivery, Recent Pat. Drug Deliv. Formul. 2 (2008) 238–257.
[6] K. Uekama, F. Hirayama, T. Irie, Cyclodextrin drug carrier systems, Chem. Rev. 98 (1998) 2045–2076.
[7] L. Perioli, C. Pagano, Inorganic matrices: an answer to low drug solubility problem, Expert Opin. Drug Deliv. 9 (2012) 1559–1572.
[8] K.K. Qian, R.H. Bogner, Application of mesoporous silicon dioxide and silicate in oral amorphous drug delivery systems, J. Pharm. Sci. 101 (2012) 444–463.
[9] C.T. Kresge, M.E. Leonowicz, W.J. Roth, J.C. Vartuli, J.S. Beck, Ordered mesoporous molecular-sieves synthesized by a liquid-crystal template mechanism, Nature 359 (1992) 710–712.
[10] M. Vallet-Regi, A. Ramila, R.P. del Real, J. Perez-Pariente, A new property of MCM-41: drug delivery system, Chem. Mater. 13 (2001) 308–311.
[11] C. Tourne-Peteilh, D.A. Lerner, C. Charnay, L. Nicole, S. Begu, J.M. Devoisselle, The potential of ordered mesoporous silica for the storage of drugs: the example of a pentapeptide encapsulated in a MSU-tween 80, Chemphyschem 4 (2003) 281–286.
[12] R. Mellaerts, R. Mols, J.A. Jammaer, C.A. Aerts, P. Annaert, J. Van Humbeeck, et al., Increasing the oral bioavailability of the poorly water soluble drug itraconazole with ordered mesoporous silica, Eur. J. Pharm. Biopharm. 69 (2008) 223–230.
[13] R. Mellaerts, C.A. Aerts, J. Van Humbeeck, P. Augustijns, G. Van den Mooter, J.A. Martens, Enhanced release of itraconazole from ordered mesoporous SBA-15 silica materials, Chem. Commun. (Camb.) 1375-7 (2007).
[14] T. Heikkila, J. Salonen, J. Tuura, N. Kumar, T. Salmi, D.Y. Murzin, et al., Evaluation of mesoporous TCPSi, MCM-41, SBA-15, and TUD-1 materials as API carriers for oral drug delivery, Drug Deliv. 14 (2007) 337–347.
[15] D. Carriazo, M. del Arco, A. Fernandez, C. Martin, V. Rives, Inclusion and release of fenbufen in mesoporous silica, J. Pharm. Sci. 99 (2010) 3372–3380.
[16] T. Limnell, E. Makila, T. Heikkila, J. Salonen, D.Y. Murzin, N. Kumar, et al., Preparation and characterization of drug formulations of ordered and nonordered mesoporous silica microparticles, Eur. J. Pharm. Sci. 44 (2011) 125–126.
[17] T. Limnell, H.A. Santos, E. Makila, T. Heikkila, J. Salonen, D.Y. Murzin, et al., Delivery formulations of ordered and nonordered mesoporous silica: comparison of three drug loading methods, J. Pharm. Sci. Us 100 (2011) 3294–3306.
[18] P. Yang, T. Deng, D. Zhao, P. Feng, D. Pine, B.F. Chmelka, et al., Hierarchically ordered oxides, Science 282 (1998) 2244–2246.
[19] D. Zhao, J. Feng, Q. Huo, N. Melosh, G.H. Fredrickson, B.F. Chmelka, et al., Triblock copolymer syntheses of mesoporous silica with periodic 50 to 300 angstrom pores, Science 279 (1998) 548–552.
[20] M. Manzano, V. Aina, C.O. Arean, F. Balas, V. Cauda, M. Colilla, et al., Studies on MCM-41 mesoporous silica for drug delivery: effect of particle morphology and amine functionalization, Chem. Eng. J. 137 (2008) 30–37.
[21] W. Stöber, A. Fink, E. Bohn, Controlled growth of monodisperse silica spheres in the micron size range, J. Colloid Interface Sci. 26 (1968) 62–69.
[22] M. Grün, I. Lauer, K.K. Unger, The synthesis of micrometer- and submicrometer-size spheres of ordered mesoporous oxide MCM-41, Adv. Mater. 9 (1997) 254–257.
[23] M. Grün, K.K. Unger, A. Matsumoto, K. Tsutsumi, Novel pathways for the preparation of mesoporous MCM-41 materials: control of porosity and morphology, Microporous Mesoporous Mater. 27 (1999) 207–216.
[24] M. Etienne, B. Lebeau, A. Walcarius, Organically-modified mesoporous silica spheres with MCM-41 architecture, New J. Chem. 26 (2002) 384–386.
[25] V. Gasparotto, I. Castagliuolo, M.G. Ferlin, 3-Substituted 7-phenyl-pyrroloquinolinones show potent cytotoxic activity in human cancer cell lines, J. Med. Chem. 50 (2007) 5509–5513.
[26] G. Viola, R. Bortolozzi, E. Hamel, S. Moro, P. Brun, I. Castagliuolo, et al., MG-2477, a new tubulin inhibitor, induces autophagy through inhibition of the Akt/mTOR pathway and delayed apoptosis in A549 cells, Biochem. Pharmacol. 83 (2012) 16–26.
[27] W.J. Xu, Q. Gao, Y. Xu, D. Wu, Y.H. Sun, W.F. Shen, et al., Controllable release of ibuprofen from size-adjustable and surface hydrophobic mesoporous silica spheres, Powder Technol. 191 (2009) 13–20.
[28] T. Heikkila, J. Salonen, J. Tuura, M.S. Hamdy, G. Mul, N. Kumar, et al., Mesoporous silica material TUD-1 as a drug delivery system, Int. J. Pharm. 331 (2007) 133–138.
[29] S. Brunauer, P.H. Emmet, E. Teller, Adsorption of gases in multimolecular layers, J. Am. Chem. Soc. 60 (1938) 309–319.
[30] E.P. Barrett, L.G. Joyner, P.P. Halenda, The determination of pore volume and area distributions in porous substances. I. Computations from nitrogen isotherms, J. Am. Chem. Soc. 73 (1951) 373–380.
[31] P.I. Ravikovitch, S.C. ODomhnaill, A.V. Neimark, F. Schuth, K.K. Unger, Capillary hysteresis in nanopores: theoretical and experimental studies of nitrogen adsorption on MCM-41, Langmuir 11 (1995) 4765–4772.
[32] P.I. Ravikovitch, D. Wei, W.T. Chueh, G.L. Haller, A.V. Neimark, Evaluation of pore structure parameters of MCM-41 catalyst supports and catalysts by means of nitrogen and argon adsorption, J. Phys. Chem. B 101 (1997) 3671–3679.
[33] E. Kaiser, R.L. Colescott, C.D. Bossinger, P.I. Cook, Color test for detection of free terminal amino groups in the solid-phase synthesis of peptides, Anal. Biochem. 34 (1970) 595–598.
[34] M. Morpurgo, D. Teoli, B. Palazzo, E. Bergamin, N. Realdon, M. Guglielmi, Influence of synthesis and processing conditions on the release behavior and stability of sol–gel derived silica xerogels embedded with bioactive compounds, Il Farmaco 60 (2005) 675–683.
[35] R. Mortera, S. Fiorilli, E. Garrone, E. Verné, B. Onida, Pores occlusion in MCM-41 spheres immersed in SBF and the effect on ibuprofen delivery kinetics: a quantitative model, Chem. Eng. J. 156 (2010) 184–192.
[36] F. Koroleff, in: G.K. KK, M. Ehrhardt (Eds.), Methods of Seawater Analysis, Wiley-VCH, Weinheim 1983, pp. 174–183.
[37] P. Falcaro, S. Costacurta, G. Mattei, H. Amenitsch, A. Marcelli, M.C. Guidi, et al., Highly ordered “defect-free” self-assembled hybrid films with a tetragonal mesostructure, J. Am. Chem. Soc. 127 (2005) 3838–3846.
[38] F. Rouquerol, J. Rouquerol, K. Sing, Adsorption by Powders and Porous Solids, Academic Press, London, 1999.
[39] M. Thommes, Physical adsorption characterization of nanoporous materials, Chem. Ing. Tech. 82 (2010) 1059–1073.
[40] M. Thommes, R. Kohn, M. Froba, Sorption and pore condensation behavior of pure fluids in mesoporous MCM-48 silica, MCM-41 silica, SBA-15 silica and controlled-pore glass at temperatures above and below the bulk triple point, Appl. Surf. Sci. 196 (2002) 239–249.
[41] C. Charnay, S. Bégu, C. Tourné-Péteilh, L. Nicole, D.A. Lerner, J.M. Devoisselle, Inclusion of ibuprofen in mesoporous templated silica: drug loading and release property, Eur. J. Pharm. Biopharm. 57 (2004) 533–540.
[42] I. Izquierdo-Barba, Á. Martinez, A.L. Doadrio, J. Pérez-Pariente, M. Vallet-Regí, Release evaluation of drugs from ordered three-dimensional silica structures, Eur. J. Pharm. Sci. 26 (2005) 365–373.
[43] B. Muñoz, A. Rámila, J. Pérez-Pariente, I. Díaz, M. Vallet-Regí, MCM-41 organic modification as drug delivery rate regulator, Chem. Mater. 15 (2003) 500–503.
[44] T. Kokubo, H. Kushitani, S. Sakka, T. Kitsugi, T. Yamamuro, Solutions able to reproduce in vivo surface-structure changes in bioactive glass-ceramic a-W^3, J. Biomed. Mater. Res. 24 (1990) 721–734.
[45] A.A. Noyes, W.R. Whitney, The rate of solution of solid substances in their own solutions, J. Am. Chem. Soc. 19 (1897) 930–934.
[46] M. Morpurgo, D. Teoli, M. Pignatto, M. Attrezzi, F. Spadaro, N. Realdon, The effect of Na(2)CO(3), NaF and NH(4)OH on the stability and release behavior of sol–gel derived silica xerogels embedded with bioactive compounds, Acta Biomater. 6 (2010) 2246–2253.